Influence of discontinuities on fatigue strength using the example of additively manufactured specimens made of AlSi10Mg

Heinz Thomas Beier [1*], *Patrick* Yadegari [1], *Michael* Vormwald[1]

[1]Technische Universität Darmstadt, Department of Civil and Environmental Sciences, Materials Mechanics Group, Franziska-Braun-Str. 3, 64287 Darmstadt, Germany

Abstract. Fatigue strength is largely affected by the influence of discontinuities: geometric notches like holes and corners in components, surface notches (roughness), pores and inclusions in the material. Therefore fatigue of structures and materials is a local problem and fatigue strength calculations are best carried out using local approaches such as local stress concept, local strain concept or fracture mechanical concepts. In this investigation, the influence of discontinuities on low cycle and high cycle fatigue strength of materials was examined on the example of additively produced material specimens made of aluminium AlSi10Mg by using a fracture mechanics parameter. Results of fatigue tests on hourglass-specimens made from four different series of 3-D printed specimens are presented. The examination of the fracture surfaces revealed that damage always started from pores located near the surface of the specimens. The fractography gave information about geometry, size and position of the crack-causing pores. The influence of such pores on the fatigue strength of the printed aluminium was investigated by using a modification of Murakami's $\sqrt{area}$ parameter. The common scatter band of the four test series could thus be reduced significantly.

1 Introduction

Additive Manufacturing (AM, 3D-printing) is a rapidly evolving manufacturing process that adds a new dimension to the traditional subtractive engineering of milling, turning and drilling. Besides other problems like process stability, repeatability, costs etc. the questions of structural integrity must be answered. Here, the topic of fatigue strength plays an important role, especially for mechanical engineering with its predominantly cyclic loads. Especially if the fatigue strength is determined by discontinuities like pores and/or inclusions, the material shows a clear scatter in fatigue strength. In this article the influence of pores on low cycle and high cycle fatigue strength of unnotched specimens made from 3-D printed aluminium is discussed on the basis of a fracture mechanics parameter.

* Corresponding author: beier@wm.tu-darmstadt.de

2 Manufacturing of hourglass specimens made of 3D-printed aluminium

The hourglass specimens were manufactured as part of the research project AddiFeE [1] to get information about the materials cyclic behaviour. The material used was an aluminium alloy AlSi10Mg (EN AC-43000, materials-no. 3.2382).

Selective laser melting (SLM) was used as the method for additive manufacturing. The machine was a Concept Laser M2 Cusing, the laser energy was 370 Watt and the island scanning pattern was used as melting strategy. No heat treatment was done after printing.

To get information about the influence of the basic process parameters on the cyclic materials behaviour 4 parameter sets were chosen (Table 1).

Table 1. Process parameter used for printing of AlSi10Mg alloy.

	P1-H3	P2-H1	P3-H4	P4-H2
volume rate	4,5 mm³/s	6,8 mm³/s	13,5 mm³/s	18 mm³/s
energy density	82,2 J/mm³	54,8 J/mm³	27,4 J/mm³	20,6 J/mm³
relative density	99,7 %	99,4 %	99,6 %	94,4 %

P2-H1 characterizes a standard parameter set with about 60 J/mm² according to Read et al. [2]. P4-H2 was chosen to produce a large number of pores. The pore-situation for all parameter sets is shown in Fig. 1.

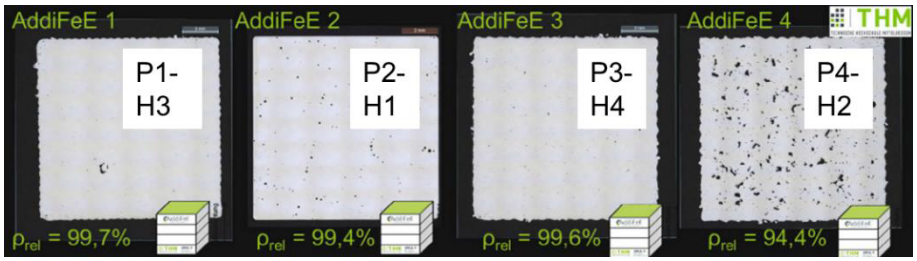

Fig. 1. 3D-printed AlSi10Mg: Pores and relative density for 4 different printing parameters.

The differences can clearly be seen: P1-H3 gives a high relative density of 99.7% with plenty of very small and a single large pore. The standard parameter set P2-H1 produces many small pores that are evenly distributed with a slightly lower relative density of 99.4%. P3-H4 has a relative density of 99.6% and a lot of very small pores. As expected, parameter set P4-H2 gives the lowest relative density of 94.4% with a lot of large pores. Obviously, the relative density gives no information about pore diameter and distribution.

In order to test the fatigue strength of the printed base material and not the influence of the printed surface, the hourglass specimens were produced in the following manner:

- Additive manufacturing of round bars d = 18 mm, l = 100 mm,
- hourglass specimen d = 6 mm made by turning and subsequent finish turning to minimize the surface roughness.

The surface of the specimens were not polished after finish turning, as pore failure could be assumed. This assumption was confirmed by the fatigue tests.

The geometry of the hourglass specimen used and a photograph of it are shown in Fig. 2. Load direction is in printing direction.

(a) (b)

Fig. 2. Hourglass specimen: (a) Geometry and dimensions. (b) Photograph, load- and printing direction.

3 Fatigue tests on AM hourglass specimen

For investigation of the influence of pores of 3D-printed specimen on cyclic materials behaviour fatigue tests were performed. The tension-compression-tests were performed on a 60 kN servo hydraulic test rig under total-strain control. The testing machine was elaborately aligned to exclude bending moments as far as possible. Fig. 3 shows the clamping area with adapter, specimen and extensometer.

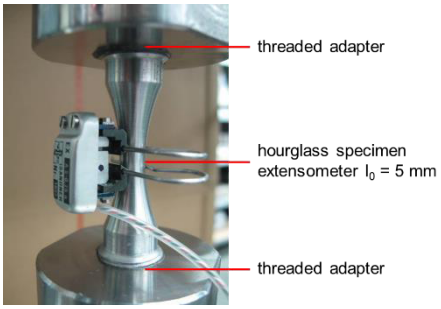

Fig. 3. Clamping of printed hourglass specimen, adapter and extensometer.

The strain ratio was set to $R_\varepsilon = -1$, the strain amplitude range was between $\varepsilon_a = 0.07$ % to 1.19 %, resulting in a number of load cycles to crack initiation of $N_i = 10^6$ to 10^2 which covers the range from high cycle to low cycle fatigue. Crack initiation life was defined at 5% quick change of maximum load.

Damage almost always started from pores close to or at the specimen surface, usually without early notice on the surface. Therefore, growth of short cracks on the specimen surface, starting with visible cracks of about 2c = 0.25 mm could not be detected. Cracks were visible from about 1 to 2 mm in length on the surface.

The fatigue life of the tested hourglass specimen made from 3D-printed AlSi10Mg was clearly determined by the crack initiating pores. Therefore, test results show a nice scatter due to the variation of geometry, size and position of these pores. Test results of all specimens tested are shown in Fig. 4 as strain amplitude versus crack initiation life. The data points are colour-coded to separate the results of the differently 3D-printed specimen. The ranking from good to not so good is: P3-H4 (green), P2-H1 (black), P1-H3 (blue) and P4-H2 (red). This corresponds with the pore pattern shown in Fig. 1. Additionally 3 lines are drawn in Fig. 4: one regression line of all test results and two lines indicating the scatter of the data.

These lines represent the strain amplitude values for 10% and 90% probability of survival $P_{s,10\%}$ (upper line) and $P_{s,90\%}$ (lower line). The scatter band is defined as the ratio between these two lines in load direction:

$$T_\varepsilon = \frac{P_{s,90\%}}{P_{s,10\%}} \quad (1)$$

The scatter of $T_\varepsilon = 1/2.67$ means a factor in lifetime of about 50.

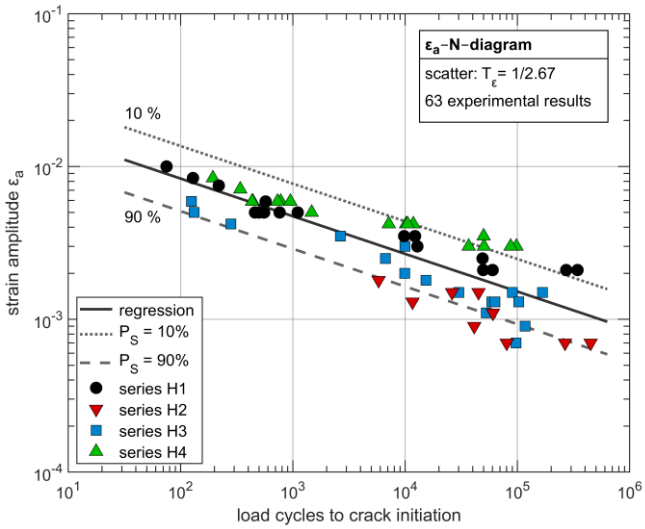

Fig. 4. Results of fatigue tests on hourglass specimen made from series H1, H2, H3 and H4 of 3D-printed AlSi10Mg.

4 Fractography of fracture surfaces

Examination of the fracture surfaces of the tested specimens provided information of the size, location and shape of the crack initiating pores in the plane perpendicular to the load direction. Since only the crack-inducing pores were examined, the data obtained should be understood in terms of extreme values. The fractographic investigation was carried out with a stereo light microscope equipped with a digital camera system and subsequent measurements were software-based. Fig 5 shows a gas pore (upper picture) and a pore resulting from not melted powder or smoke residue (lower picture), together with the dimensions length a, width b and distance to surface c. From these values the area of the pores was then calculated using ellipses and additionally by measure of the pore boundaries. Using the different methods of area calculation did not have much influence on the results of the subsequent calculations.

The results of the fractographic investigation are shown in Fig. 6 exemplarily as a diagram of the cumulative frequency for the maximum length *a* of crack initiating pores. The diagram is colour-coded again for comparison with Fig. 4. The mean values (not: median) of the maximum length *a* are in ascending order: 140 µm (P3-H4, green), 240 µm (P2-H1, black), 720 µm (P1-H3, blue) and 840 µm (P4-H2, red). The results for maximum length *b* and calculated *area* are similar. The order corresponds to the ranking determined in the fatigue tests, see Fig. 4.

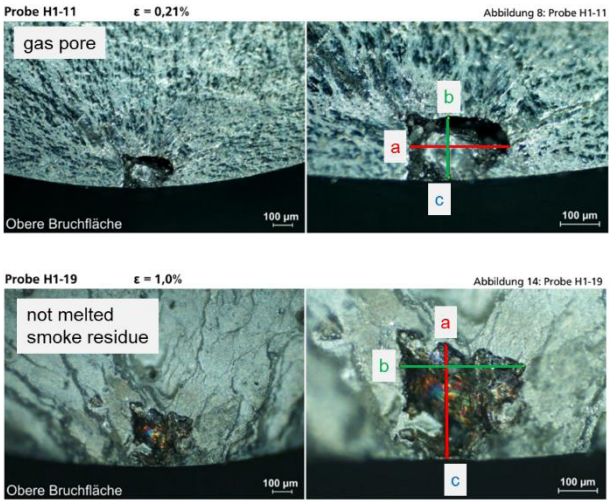

Fig. 5. Fracture surface of 3D-printed AlSi10Mg specimen: Crack initiating pores and dimensions length a, width b and distance to surface c.

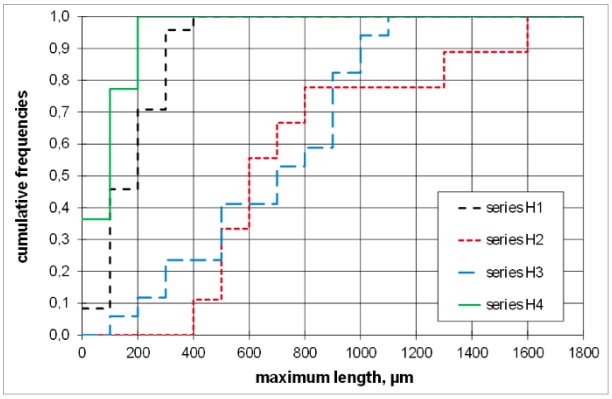

Fig. 6. Cumulative frequency for the maximum length a of crack initiating pores of 3D-printed AlSi10Mg specimen.

5 Computer tomography of specimen volume

Computer tomography (CT) scans for 10 of the tested specimens were done before cyclic testing for the series P4-H2 only, Fig. 7. The aim of this investigation was to find the crack initiating pores, measurement of their geometry and correlation with the results from fractography.

The CT scans and delivery of huge amounts of data were carried out by colleagues at Chair and Institute for Materials Technology (IfW) at TU Darmstadt. The very complex evaluation of the 3D data was carried out in part with the open source software ImageJ2 [3]. As a result the crack initiating pores from chapter 4 could be found and separated to measure their size, but – in our case – not predicted. One reason for this is the large number of several possible fracture origins of almost the same dimension.

A comparison of the data got from fractography and CT examinations can be found in Table 2. The values agree very well.

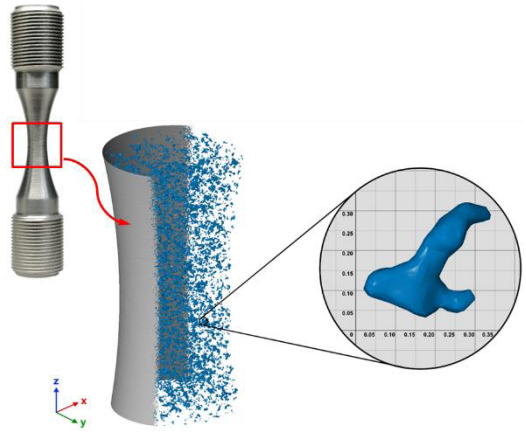

Fig. 7. CT scan for testing area of 3D-printed AlSi10Mg specimen from test series P4-H2.

Table 2. Comparison of mean value results from fractography and computer tomography for the crack initiating pores of test series P4-H2.

crack initiating pore	length a mean value µm	width b mean value µm	distance to surface c mean value µm
fractography	840	407	5
computer tomography	805	428	11

6 Influence of pores on fatigue strength

Obviously the fatigue strength of the tested 3D-printed aluminium AlSi10Mg is mainly determined by the actual pore situation. There is no competition between microstructure and pores, because the pores every time win the race. In such a case, it is not necessary to correlate the fatigue strength with microstructural parameters.

For the chosen fracture mechanics based approach the pore is considered as a crack-like defect. The influence of pores on fatigue strength was then investigated by using a modification of Murakami's $\sqrt{area}$ parameter to approximate the maximum stress intensity factor for more or less arbitrarily shaped crack geometries [4]:

$$K_{\mathrm{I,max}} = 0.65\sigma\sqrt{\pi\sqrt{area}} \tag{2}$$

The value of $area$ is calculated using the pore dimensions determined in chapter 4. The value of 0.65 is used for surface cracks and cracks close to the surface, for internal cracks it would be 0.50. The formula is valid in linear elastic fracture mechanics.

The Murakami parameter was modified for low cycle fatigue by introducing El Haddad's strain based crack tip parameter K_{ε} [5] (in short: strain intensity factor) in terms of amplitudes:

$$K_{\varepsilon,\mathrm{a}} = 0.65\varepsilon_{\mathrm{a}}\sqrt{\pi\sqrt{area}} \cdot f \tag{3}$$

$K_{\varepsilon,a}$ was calculated under consideration of the elastic-plastic strain amplitudes ε_a, which easily could be taken from test data of the total strain controlled experiments. Otherwise it can be calculated by elastic-plastic analysis such as finite element method or Neuber's formula etc. An extrapolated geometry function f from Shah and Kobayashi [6] was added, to better take the position of the pores relative to the specimen surface into account.

A re-evaluation of the test data from chapter 3 using this approach then leads to a significant reduction of the scatter. For calculation of K_ε the parameter $area$ was calculated by ellipse. A comparison of the ε-N-diagram and the K_ε-N-diagram together with the scatter band T_ε for all tested specimens made with the different parameter sets for AM is shown in Fig. 8.

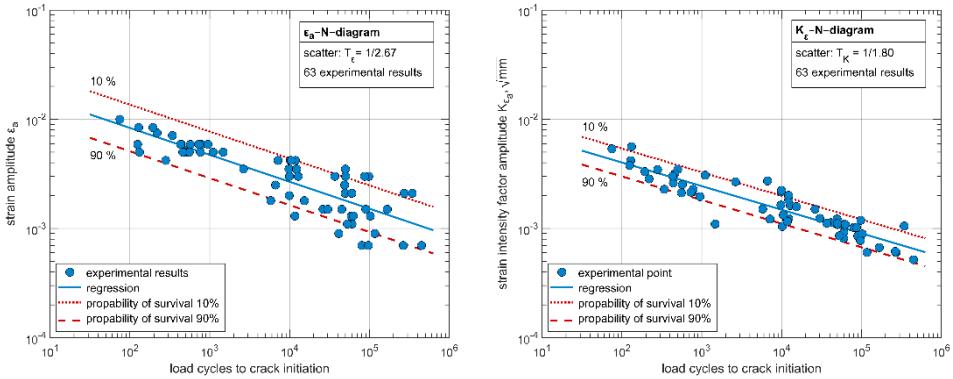

(a) (b)

Fig. 8. Results of fatigue tests on hourglass specimen made from series H1 to H4 of 3D-printed AlSi10Mg. (a): total strain versus number of cycles to crack initiation. (b): strain intensity factor versus number of cycles to crack initiation. The slope of the regression lines is $m = 4.06$ for case (a) and $m = 4.63$ for case (b).

The scatter band reduces from $T_\varepsilon = 1/2.67$ to $T_\varepsilon = 1/1.80$ which means a reduction of scatter in number of load cycles by a factor of about 4.

7 Summary and Conclusion

Hourglass specimens were made from 3D-printed bars made of AlSi10Mg. Four different parameter sets for additive manufacturing were used to get different pore situations. Strain controlled fatigue tests were carried out to get information of the influence of pores on fatigue life. When all test results are evaluated together, there is a clear scatter band in the strain Wöhler curve.

A fractographic examination of the fracture surfaces provided information of the size, position and shape of the crack initiating pores. Data of CT scans made prior to fatigue tests could be correlated to these results.

To take into account the influence of pores on the fatigue strength, a fracture mechanics based approach was used: Murakami's $area$ parameter together with El Haddad's strain based crack tip parameter K_ε. For a better consideration of the pore distance to the surface a geometry function of Shah-Kobayashi was used.

As a result a significant reduction of scatter could be achieved when all test results were evaluated together again. The influence of pores on the fatigue strength is thus basically determined correctly.

If appropriate information about pores is available (non-destructive testing, computer tomography, high resolution ultrasonic testing), this easy engineering approach may be used to improve estimation of fatigue strength of structures containing discontinuities like pores or inclusions.

Acknowledgements for the production of the specimens and the fatigue tests : This project (HA Project No .: 464 / 15-06, AddiFeE) was as part of Hessen ModellProjekte funded by LOEWE - State Offensive for Development of Scientific and economic Excellence, Funding line 3: SME collaborative projects funded.

References

1. U. Jung, *AddiFeE – Innovation additive Fertigung*, LOEWE research project HA 464/15-06, HessenAgentur (2017)
2. N. Read, W. Wang, K. Essa, M.M. Attallah, Mater. Des., **65**, 417 (2015)
3. C.T. Rueden, J. Schindelin, M.C. Hiner, B.E. DeZonia, A.E. Walter, E.T. Arena, K.W. Eliceiri, BMC Bioinform., **18**, 529 (2017). doi:10.1186/s12859-017-1934-z
4. Y. Murakami, *Effects of Small Defects and Nonmetallic Inclusions*. ISBN 0-08-044064-9, Elsevier Science Ltd., Oxford, 2002, pp. 11-24 (2002)
5. M. El Haddad, K.N. Smith, T.H. Topper, *A Strain Based Intensity Factor Solution for Short Fatigue Cracks Initiating from Notches,* in Proceedings of the Eleventh National Symposium on Fracture Mechanics: Part I, edited by Smith, PA: ASTM International, 1979, 274-289, (1979)
6. R.C. Shah, A.S. Kobayashi, Int. J. Fract., **9**, 133 (1973)